

Effects of Alkali Cations and Halide Anions on the Self-Assembly of Phosphatidylcholine in Oils

Shih-Ting Lin,[†] Chen-Shin Lin,[†] Ya-Ying Chang,[†] Andrew E. Whitten,[‡] Anna Sokolova,[‡] Chun-Ming Wu,^{§,‡} Viktor A. Ivanov,^{||} Alexei R. Khokhlov,^{||} and Shih-Huang Tung^{*,†}

[†]Institute of Polymer Science and Engineering, National Taiwan University, Taipei 10617, Taiwan

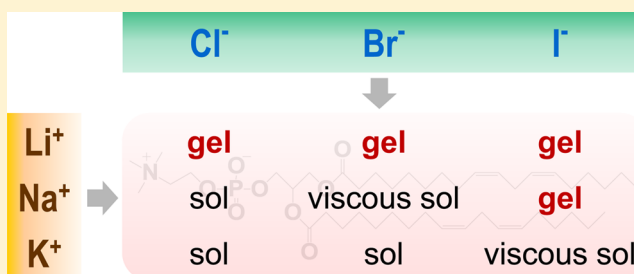
[‡]Australian Nuclear Science and Technology Organisation, Lucas Heights, NSW 2234, Australia

[§]National Synchrotron Radiation Research Center, Hsinchu 30076, Taiwan

^{||}Faculty of Physics, Moscow State University, Moscow 119991, Russia

Supporting Information

ABSTRACT: The interactions between ions and phospholipids are closely associated with the structures and functions of cell membrane. Instead of conventional aqueous systems, we systematically investigated the effects of inorganic ions on the self-assembly of lecithin, a zwitterionic phosphatidylcholine, in cyclohexane. Previous studies have shown that addition of inorganic salts with specific divalent and trivalent cations can transform lecithin organosols into organogels. In this study, we focused on the effect of monovalent alkali halides. Fourier transform infrared spectroscopy was used to demonstrate that the binding strength of the alkali cations with the phosphate of lecithin is in the order $\text{Li}^+ > \text{Na}^+ > \text{K}^+$. More importantly, the cation–phosphate interaction is affected by the paired halide anions, and the effect follows the series $\text{I}^- > \text{Br}^- > \text{Cl}^-$. The salts of stronger interactions with lecithin, including LiCl , LiBr , LiI , and NaI , were found to induce cylindrical micelles sufficiently long to form organogels, while others remain organosols. A mechanism based on the charge density of ions and the enthalpy change of the ion exchange between alkali halides and lecithin headgroup is provided to explain the contrasting interactions and the effectiveness of the salts to induce organogelation.



1. INTRODUCTION

Phospholipids are the main components in cell membranes.¹ Since cell membranes are physiologically in contact with electrolyte solutions, the interplays between phospholipids with ions have drawn much attention. It has been shown by experiments^{2–7} and simulations^{8–11} that the structure, dynamics, and stability of phospholipid bilayers are affected by ions. Ions can change headgroup tilt and tail ordering to force the lipids more closely packed, which in turn increases the rigidity as well as decreases the lateral diffusion coefficient and water permeability of the membranes.^{8,12,13} In addition, ions are known to regulate processes such as protein binding and insertion, membrane fusion, and gating of ion channels, which are essential for the functioning of cells.^{14–17} In general, the observed effects are ion-specific, dependent on ion size, valency, and polarizability, and mostly follow the well-known Hofmeister series.^{18,19}

The specific binding of cations to phospholipids has been studied in a variety of aqueous systems, including the bilayers formed by both negatively charged and zwitterionic phospholipids. These cations mainly associate with the negatively charged phosphate of the headgroups.^{2,8} It has been found that the binding affinity of cations to phospholipids in water follows the order $\text{La}^{3+} > \text{Ca}^{2+} > \text{Na}^+$, consistent with the order of

valence.^{2,4,10} However, even if the valency of the cations is the same, the affinity may be different. For example, among divalent cations, Ca^{2+} has the strongest binding affinity, and the affinity of La^{3+} is lower than that of Ce^{3+} .^{4,5} In contrast, fewer studies have focused on the influence of anions on lipid bilayers. For the common halide anions which mainly interact with the positively charged choline group on phosphatidylcholines, the adsorption to membranes was found to follow series $\text{I}^- > \text{Br}^- > \text{Cl}^- > \text{F}^-$.^{10,20,21} Anions with a large size, such as I^- , show a higher affinity for the membrane and penetrate more deeply into the bilayer interior than small anions.^{11,22,23} It has also been found that the interaction of anions with phospholipids is affected by the types of counterions. For example, the adsorption of Cl^- to bilayers weakens when Na^+ is replaced by K^+ as the counterion.²⁵

To account for the ion–ion interactions in water, two classes of ions can be distinguished based on the strength of ion–water interaction.^{24,25} Small ions of high charge density that interact strongly with water are called kosmotropes while large monovalent ions of low charge density that show a weak

Received: September 20, 2016

Revised: October 31, 2016

Published: November 1, 2016

interaction with water are called chaotropes. In aqueous systems, the formation of the kosmotrope–kosmotrope ion pair is energetically favorable because the distance between the two charges of opposite sign is shorter. Although the interaction between chaotropes with opposite sign in a vacuum is weak, chaotrope–chaotrope ion pairs are energetically favorable in water as well. The reason is that the formation of chaotrope–chaotrope pairs can release water molecules for forming more water–water interactions that are stronger than chaotrope–water ones. This is similar to the well-known “like dissolves like” phenomenon.²⁴ This rule can explain the order $\text{La}^{3+} > \text{Ca}^{2+} > \text{Na}^+$ (charge density from high to low) to bind phosphate group (a kosmotrope) and the order $\text{I}^- > \text{Br}^- > \text{Cl}^- > \text{F}^-$ (charge density from low to high) to interact with choline group (a chaotrope) in water.

Apart from the aqueous systems, we have previously reported that ions can modulate the self-assembly of lecithin, a zwitterionic phospholipid (Figure 5), in low polar organic solvents (oils), too.²⁶ Inorganic salts like CaCl_2 and LaCl_3 cannot be dissolved in oil alone. However, small amounts of salts can be dissolved in oil when lecithin is present. The dissociated ions bind the phosphocholine headgroups of lecithin and induce a transition from spherical reverse micelles to cylindrical micelles. The lengths of the cylindrical micelles have been suggested to exceed several hundred nanometers so that these long, robust micelles give rise to a quasi-permanent gel network, unlike the conventional viscoelastic wormlike micelles formed by lecithin and other additives, such as water and bile salts, in oils.^{27–30} Interestingly, the effectiveness on organogel formation correlate with the binding affinities of cations with phospholipids in water as described above; that is, organogelation is induced by La^{3+} and Ca^{2+} but not by Na^+ when paired anions are all Cl^- .

The previous study shows that only divalent and trivalent cations can induce the lecithin organogels and the role of the counterions has not yet been discussed.²⁶ In this study, we systematically investigated on the effects of a series of alkali halides on the self-assembly of lecithin in cyclohexane. Even though all the cations and anions are monovalent, the abilities of the salts to induce gels are apparently different, and some of the salts can indeed lead to organogels. We utilized rheological and small-angle neutron scattering techniques to examine the flow properties and the structures of the reverse micelles. We find that not only alkali cations take effect but halide anions also play significant roles in the gel formation. Coincidentally, the effectiveness of the cations to induce gel decreases with decreasing charge density, $\text{Li}^+ > \text{Na}^+ > \text{K}^+$, and the effectiveness of the anions decreases with increasing charge density, $\text{I}^- > \text{Br}^- > \text{Cl}^-$, consistent with Hofmeister series found in aqueous solutions even though the amount of water in these oil systems is negligible.¹⁸ Among the salts, LiCl , LiBr , LiI , and NaI can induce lecithin organogels whereas others cannot. Fourier transform infrared (FTIR) spectroscopy was used to investigate the interactions between lecithin and alkali halides,³¹ which unambiguously shows the strengths of interactions follow the above orders.

One advantage of the oil systems is that the low polar solvents provide a nearly water-free platform that can elucidate the strengths and the binding sites of the intermolecular interactions without the disturbance of water, which is useful for understanding the physiological process in human bodies. In practical aspect, the formulas found in this work can be used

for rheological control of oils.³² In addition, the organogels are highly potential for biomedical applications.

2. EXPERIMENTAL SECTION

2.1. Materials. Soybean lecithin (95% purity) was purchased from Avanti Polar Lipids, Inc. Alkali halides were in anhydrous form, and the purities were higher than 99%. The purities of the solvents, including methanol and cyclohexane, were higher than 99.5%. The deuterated cyclohexane with purity 99.6% was purchased from Sigma-Aldrich. All chemicals were used as received.

2.2. Sample Preparation. Lecithin and alkali halides were dissolved in methanol to form 100 mM stock solutions. The molar ratio of salt to lecithin was adjusted by mixing appropriate amounts of the stock solutions. After mixing, methanol was removed by drying the samples in a vacuum oven at 50 °C for 48 h. The final samples with desired concentrations were obtained by adding proper amounts of cyclohexane, followed by stirring and sonication until the solutions were well mixed.

2.3. Rheological Studies. Steady-shear and dynamic rheological experiments were performed on an AR2000EX stress-controlled rheometer (TA Instruments). Different sample holders were used, including cone-and-plate, parallel plate, and concentric cylinder geometry, depending on the flow properties of samples. All samples were studied at 25 ± 0.1 °C, and a solvent trap was used to minimize evaporation of cyclohexane. Dynamic frequency spectra were conducted within the linear viscoelastic regime. For steady-shear experiments, sufficient time was allowed before data collection at each shear rate to ensure that the viscosity reached its steady-state value.

2.4. Small-Angle Neutron Scattering (SANS). SANS measurements were made on Bilby beamline at ANSTO in Sydney, Australia, which is operated in time-of-flight data collection mode.³³ Neutrons with a range of wavelengths from 2 to 18 Å ($\Delta\lambda/\lambda = 8.3\%$) were used to cover a q -range from 0.003 to 0.4 Å⁻¹. Samples were diluted to 20 mM of lecithin in deuterated cyclohexane and studied in 1 mm quartz cells at 25 °C. The data are shown as plots of the absolute intensity I versus the wave vector $q = 4\pi \sin(\theta/2)/\lambda$, where λ is the wavelength of neutrons and θ is the scattering angle.

2.5. SANS Modeling. Modeling of SANS data was conducted using the package provided by NIST and run with the IGOR Pro software.³⁴ For dilute solutions of noninteracting scatterers, the SANS intensity $I(q)$ can be modeled in terms of the form factor $P(q)$ of the scatterers. In this study, form factor models for ellipsoids and cylinders with polydisperse length were considered, as described below.

2.5.1. Ellipsoids. The form factor $P(q)$ for ellipsoids of revolution with minor and major axes R_a and R_b is given by³⁵

$$P(q) = (\Delta\rho)^2 \left(\frac{4}{3} \pi R_a R_b^2 \right)^2 \int_0^1 \left[3 \frac{\sin x - x \cos x}{x^3} \right]^2 d\mu \quad (1)$$

where

$$x = q \sqrt{\mu^2 R_b^2 + R_a^2 (1 - \mu^2)} \quad (2)$$

Here $\Delta\rho$ is the difference in scattering length density between the scatterer and the solvent. $(\Delta\rho)^2$ is thus the scattering contrast. μ is the cosine of the angle between the wave vector q and the symmetry axis of the ellipsoid.

2.5.2. Cylinders with Polydisperse Length. The form factor $P(q)$ for cylinders of radius R_c and length L is given by³⁵

$$P(q) = (\Delta\rho)^2 (\pi R_c^2 L)^2 \int_0^{\pi/2} [F(q, \alpha)]^2 \sin \alpha d\alpha \quad (3)$$

where

$$F(q, \alpha) = \frac{J_1(q R_c \sin \alpha) \sin(q L \cos \alpha/2)}{(q R_c \sin \alpha) (q L \cos \alpha/2)} \quad (4)$$

Here α is the angle between the wave vector q and the cylinder axis. $J_1(x)$ is the first-order Bessel function of the first kind. For the

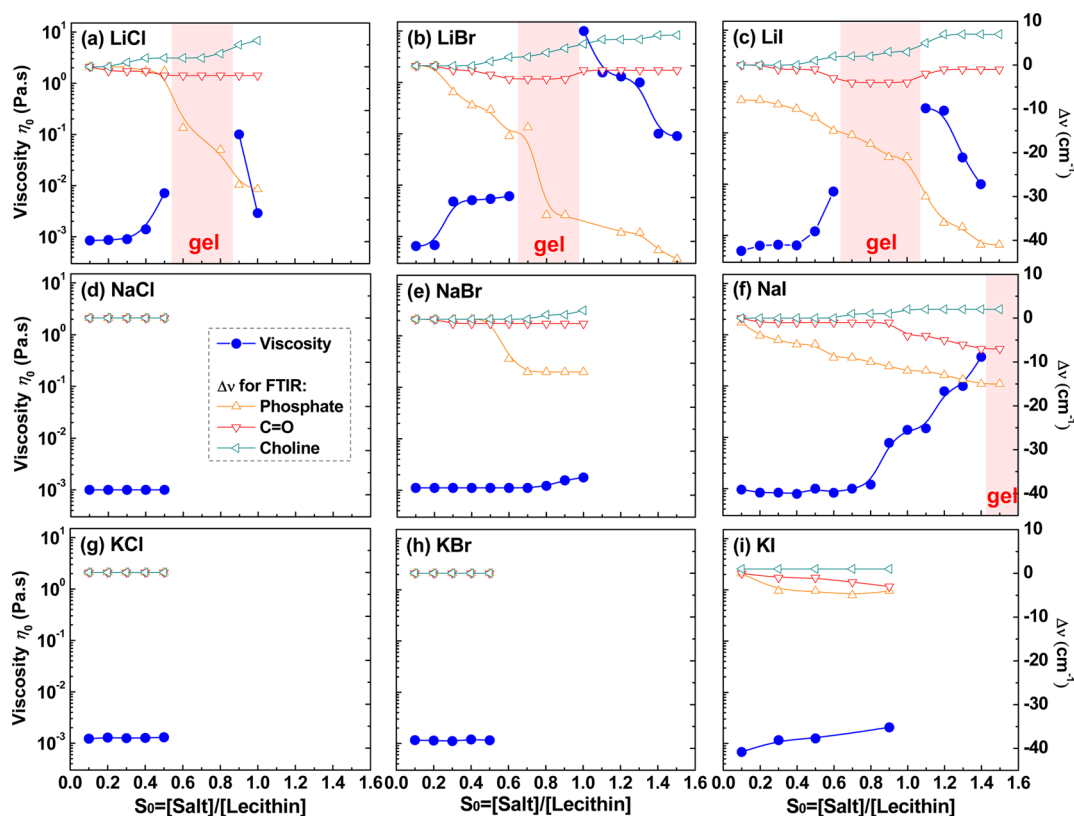


Figure 1. Zero-shear viscosity η_0 of alkali halide/lecithin in cyclohexane at 25 °C and FTIR band shift ($\Delta\nu$) of phosphate, carbonyl, and choline group on lecithin as functions of S_0 , the molar ratio of alkali halide to lecithin. The lecithin concentration is fixed at 100 mM. Only the data from homogeneous samples are shown in the plots. Organogels are formed in the regions filled with red color, where η_0 cannot be obtained due to the lack of viscosity plateau at low shear rate.

cylinders with polydisperse length, the form factor is averaged over the length distribution:

$$P(q) = \int f(L)P(q, L) dL \quad (5)$$

where $P(q, L)$ is the form factor for a cylinder of length L (eq 3). The polydispersity in cylinder length $f(L)$ is described by the Schulz distribution:

$$f(L) = \left(\frac{z+1}{L_0}\right)^{z+1} \frac{L^z}{\Gamma(z+1)} \exp\left(-\frac{z+1}{L_0}L\right) \quad (6)$$

where L_0 is the average cylinder length and Γ is the gamma function. The polydispersity index p_d is defined by

$$p_d = \frac{1}{\sqrt{z+1}} \quad (7)$$

2.6. Fourier Transform Infrared Spectrometer (FTIR). FTIR spectra were recorded in transmission mode with a PerkinElmer Spectrum 100 model FTIR spectrometer. Samples of 100 mM lecithin with different molar ratio of alkali halides in cyclohexane were loaded into a CaF_2 cell (0.05 mm thickness) and analyzed over a range of wavenumbers from 4000 to 950 cm^{-1} at 25 °C. Each spectrum was collected under an accumulation of 16 scans at 1 cm^{-1} resolution. Pure solvents in the CaF_2 cell were taken as background references before measuring the spectra of samples.

3. RESULTS AND DISCUSSION

3.1. Phase Behaviors and Rheological Properties. We first discuss the dependence of alkali halide/lecithin molar ratio, denoted as S_0 , on the rheological properties of the mixtures in cyclohexane. The alkali cations used in this work include

lithium (Li), sodium (Na), and potassium (K), and the halide anions include chlorine (Cl), bromine (Br), and iodine (I). Lecithin alone in low polar solvent forms reverse ellipsoidal micelles that are nearly spherical,^{26,28} and the viscosity at 100 mM is almost as low as that of cyclohexane. All the salts are unable to dissolve in cyclohexane alone but become soluble at a limited amount when lecithin is present. Although all the salts are composed of monovalent ions, they show different effects on the phase behaviors and rheological properties of lecithin solutions.

The zero-shear viscosities η_0 as functions of S_0 for all the alkali halide/lecithin mixtures are shown as the blue curves in Figure 1. The lecithin concentration was fixed at 100 mM. In Figure 1a, the LiCl/lecithin mixtures reveal the general behavior for gel-inducing salts. At $S_0 < 0.3$, the viscosity is as low as that of cyclohexane. The lecithin micelles at low S_0 remain about spherical, and the viscosity is unaffected. At $S_0 > 0.3$, η_0 increases rapidly and becomes immeasurable, i.e., no viscosity plateau found at low shear rate, in a narrow S_0 range between 0.6 and 0.8 where the solution stops flowing in the inverted vial, typical of gels with a solidlike behavior. It has been suggested that the spherical micelles are transformed into long, entangled cylindrical micelles with a very long relaxation time.²⁶ The salt in this range is completely dissolved, and the organogel looks optically transparent. As S_0 keeps increasing, η_0 drops sharply and the sample becomes a thin, clear liquid with a viscosity close to that of solvent at $S_0 \sim 1.0$, implying that the long cylindrical micelles turn into short ones. Furthermore, LiCl is about saturated at $S_0 \sim 1.0$, above which the excess LiCl

gives rise to a phase separation and the samples become cloudy. The phase-separated samples were not further studied.

The viscosity changes of LiBr and LiI mixtures with S_0 are similar to that of LiCl. The differences are that the range of gel is slightly higher, 0.7–0.9 for LiBr and 0.7–1.0 for LiI, and phase separation occurs at a higher S_0 , ~ 2.0 for LiBr and ~ 2.5 for LiI. NaI is another salt capable of inducing organogel. However, the range of gel ($S_0 \sim 1.5$ –1.6) is much higher than those of lithium salts, and at $S_0 > 1.6$, phase separation occurs directly, without the homogeneous, low-viscous regime found in lithium salts. In contrast, for the rest of alkali halides, phase separation occurs at relatively low S_0 , ~ 1.0 for NaBr and KI and 0.5 for NaCl, KCl, and KBr. It is apparent that the binding strengths of these salts are weaker than those of the gel-inducing salts. NaBr and KI can slightly enhance the viscosity whereas NaCl, KCl, and KBr have no effect on the viscosity before phase separation.

Comparing the viscosity data of the alkali halides used in this work, the capability of the alkali cations to induce the formation of lecithin cylindrical micelles is in the order $\text{Li}^+ > \text{Na}^+ > \text{K}^+$. In addition to the cations, we noticed that the halide anions also play a significant role. For the most capable Li^+ , the salts with all the three anions can cause the gelation, whereas for the least capable K^+ , no matter what anions are paired, the salts are unable to induce gels before phase separation. Interestingly, in the case of sodium salts, NaI can lead to the gel, whereas NaBr only slightly increases the viscosity and NaCl has no influence on the viscosity at all. The results imply that the capability of the halide anions to induce the growth of cylindrical micelles is in the order $\text{I}^- > \text{Br}^- > \text{Cl}^-$. The ability of the salts to transform the micellar shape and rheology is dependent on the strengths of intermolecular interactions between lecithin and the salts, which will be discussed in the FTIR section.

The viscoelasticity of the organogels was characterized by dynamic rheology. The elastic modulus (G') and the viscous modulus (G'') as functions of frequency ω for the samples containing 100 mM lecithin mixed with LiCl, LiBr, LiI, and NaI in their gel ranges, $S_0 = 0.7, 0.7, 0.7,$ and 1.6 respectively, are shown in Figure 2. All of the samples exhibit a dominance of G'

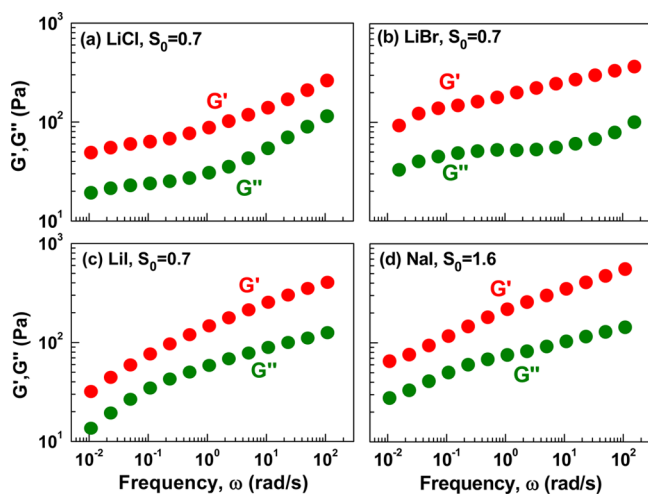


Figure 2. Dynamic rheology of the organogels at 25 °C. The samples contain 100 mM lecithin in cyclohexane, and S_0 's for LiCl, LiBr, LiI, and NaI are 0.7, 0.7, 0.7, and 1.6, respectively, all in gel range. The plots show elastic modulus G' and viscous modulus G'' as functions of frequency ω .

over G'' across the entire frequency range, implying an elastic response of the samples. The moduli, however, are weakly frequency-dependent, and the difference between G' and G'' becomes narrower at low frequencies. Note that the G' and G'' curves do not intersect, which indicates that the relaxation times of the samples are very long and fall outside the window of time scales probed by the rheometer.³⁶ Since a true gel that has infinite values of relaxation time and zero-shear viscosity would show frequency-independent moduli over the entire frequency range, the above response is regarded as gel-like.³⁷ Such weak gels behave like an elastic solid when they are observed in a practical time scale.

3.2. SANS. SANS was utilized to probe the self-assembled structures of the alkali halide/lecithin in deuterated cyclohexane. The lecithin concentration of the samples was fixed at a relatively low 20 mM to eliminate the contribution from the structure factor caused by intermicellar interactions. The SANS profiles of the representative LiI/lecithin samples with varying S_0 are shown in Figure 3. The data have been rescaled by

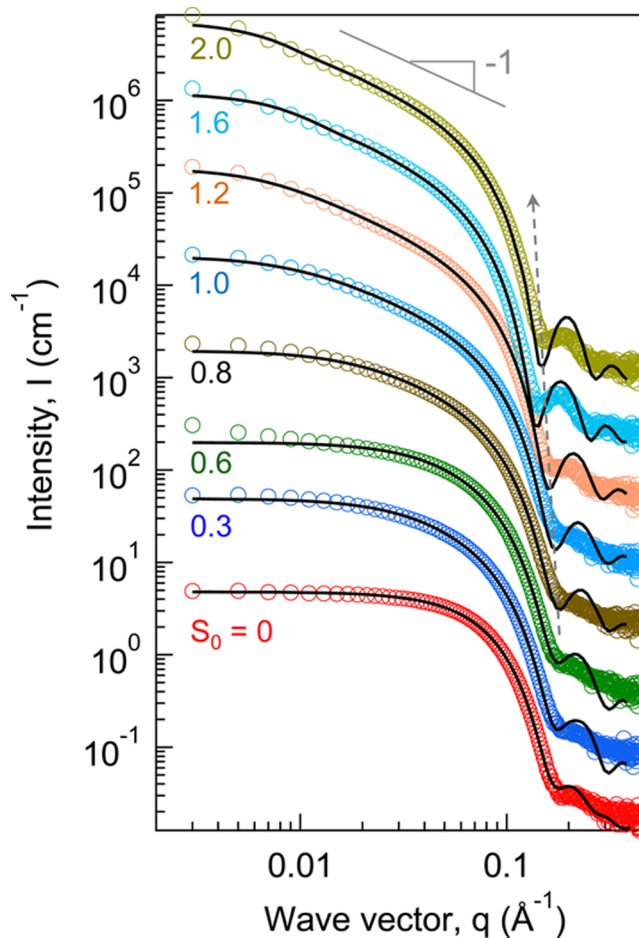


Figure 3. SANS data for LiI/lecithin in deuterated cyclohexane containing 20 mM lecithin at various S_0 . The data are separated by factors of 5. Model fits are shown as solid lines through each curve.

factors of 5 for clarity purpose. The profile of pure lecithin sample ($S_0 = 0$) is nearly flat in low q range, which is typical of spheroidal structure. The intensity at low q increases with increasing S_0 , indicating a growth of micelles as the amount of LiI increases. For $S_0 > 1.0$, the profiles show a $I \sim q^{-1}$ power-law behavior in the intermediate q range, which is a scaling

relationship expected for cylindrical structures.³⁵ The structural transformation of the micelles from spheroids into cylinders induced by LiI is thus qualitatively evidenced. In addition to the change of the intensity in the low q range, the turning points of the profiles around $q = 0.1 \text{ \AA}^{-1}$ show a subtle but meaningful dependence on S_0 . The downturn here reflects the shorter characteristic length of the structures, i.e., the radius of the spheroidal or the cylindrical micelles in the present case. As S_0 increases, the profile drops at a lower q , implying LiI causes the radius of the micelles to increase. The SANS data therefore demonstrate that the incorporation of LiI into lecithin sols can induce both the axial and radial growth of the micelles.

To quantify the change of micellar sizes, we model the SANS data of LiI/lecithin mixtures using appropriate form factors, as described in section 2.5. The fits are shown as the solid curves through the rescaled data in Figure 3. For pure lecithin in cyclohexane ($S_0 = 0$), the micelles are modeled as oblate ellipsoids of revolution (eqs 1 and 2) with radii of 20.4 and 30.6 Å for their minor and major axes. Such an oblate ellipsoid is approximately spherical.²⁸ Upon addition of LiI, the micelles grow axially, and the model for cylinders with polydisperse length (eqs 3–7) is used. At $S_0 = 0.3, 0.6,$ and 0.8 , the micelles may be in the transition state, and the cylinder models show deviations from the profiles in low q range. At $S_0 > 1.0$, the data can then be fit reasonably well for the whole q range. Polydisperse cylinder parameters from the modeling are listed in Table 1. From the fitting parameters, it is found that the

Table 1. Fitting Parameters of Cylinders with Polydisperse Length for SANS Data of LiI/Lecithin Mixtures Shown in Figure 3

[LiI]/[lec] (S_0)	R_c (Å)	L_0 (Å)	p_d
0.3	23.1	58.9 ± 0.5	0.69
0.6	23.3	51.3 ± 0.5	0.59
0.8	22.4	101.2 ± 0.7	0.68
1.0	22.8	194.4 ± 1.6	0.71
1.2	24.0	395.4 ± 3.3	0.44
1.6	27.5	489.2 ± 2.7	0.01
2.0	26.0	598.3 ± 1.3	0.01

average length of cylinders (L_0) greatly increases with S_0 , and simultaneously, the radius of the cylinders (R_c) increases from 22–23 Å at $S_0 < 1.0$ to 26–27 Å at $S_0 > 1.6$, confirming the axial and radial growth of the micelles and the formation of long cylindrical micelles in the gel samples. Note that the length of the micelles at $S_0 > 1.2$ is longer than that in the gel range ($S_0 = 0.7–1.0$ for LiI), which is not consistent with the rheological data shown in Figure 1c where the viscosity sharply drops at $S_0 \geq 1.1$. It is possible that the different concentrations used for SANS experiments (20 mM) and rheological measurements (100 mM) cause a shift of S_0 .

The SANS data and model fittings of other gel-inducing salts, LiCl, LiBr, and NaI, are shown in Figures S1–S3 of the Supporting Information. The effects of these salts on lecithin micellar structure are similar; that is, the length of the cylindrical micelles keeps increasing as S_0 increases, even above the range of gel. The representative SANS data and model fittings of the non-gel-inducing salts, including NaBr, KCl, and KI, are shown in Figures S4–S6. All the salts can slightly increase the size of the micelles, but the samples phase separate prior to the formation of sufficiently long micelles that are able to gel the solutions.

3.3. FTIR. Rheology and SANS data have shown that some specific alkali halides can induce the growth of long reverse cylindrical lecithin micelles that bring about organogels while others cannot. In this section, we use FTIR techniques to clarify how the alkali cations and halide anions interact with the phosphate, carbonyl, and choline group on lecithin (see Figure 5 for the chemical structure). The representative FTIR spectra of LiCl/lecithin mixtures are shown in Figure 4 while others are

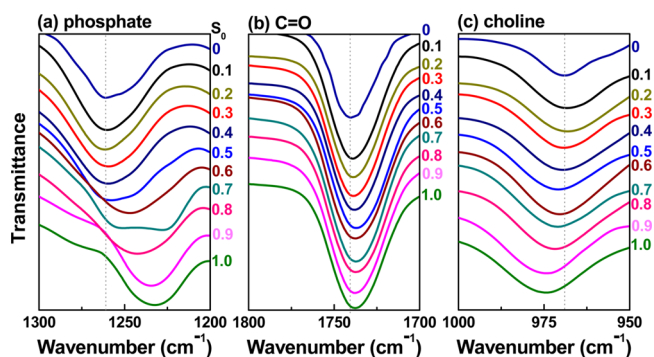


Figure 4. FTIR absorption bands of (a) phosphate, (b) carbonyl group C=O, and (c) choline on lecithin for LiCl/lecithin at various S_0 in cyclohexane at 25 °C. The lecithin concentration is 100 mM. The band shifts ($\Delta\nu$) as functions of S_0 are displayed in Figure 1a.

shown in Figures S7–S14. The changes of the absorption bands

($\Delta\nu$) as functions of S_0 for all the salts are displayed in Figure 1,

which can be conveniently compared to the viscosity data.

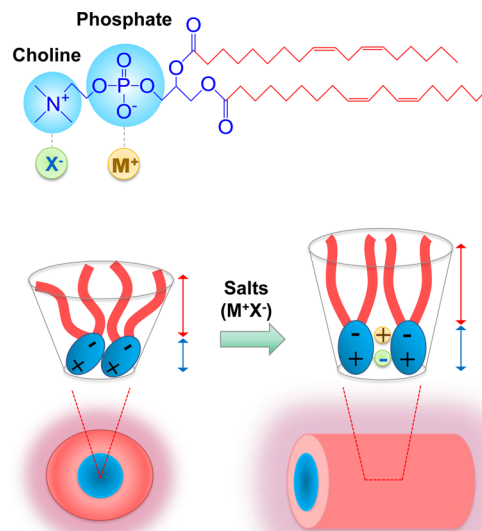


Figure 5. Top panel shows the structure of lecithin where alkali cations (M^+) bind to the phosphate while halide anions (X^-) bind to the choline of the headgroup. The bottom left panel reveals that lecithin alone with tilt headgroup and swollen tails has a conical shape in cyclohexane and forms discrete, nearly spherical reverse micelles. The bottom right panel depicts ions binding to lecithin, causing the lipid tails to be more straightened and the tail area to shrink. The molecular geometry becomes more like a truncated cone that favors cylindrical micelles, thereby converting the sample into an organogel. The straightened tails and headgroup explain the radius growth of the micelles as S_0 increases.

3.3.1. Phosphate Group. The primary site on lecithin headgroups that interact with other polar or ionic compounds is the phosphate group (PO_4^-).³⁸ It has been reported that the band of the asymmetric stretching of phosphate on lecithin in low polar organic solvents is near 1260 cm^{-1} , and it shifts to a lower wavenumber (a red-shift) upon hydrogen bonding.³⁹ Figure 4a shows that pure lecithin in cyclohexane ($S_0 = 0$) gives a main phosphate absorption band at 1261 cm^{-1} . A shoulder around 1250 cm^{-1} results from the phosphate groups hydrogen bonded with a trace of water that is unable to be removed by drying.²⁸ When LiCl dissolves in lecithin organosols, it dissociates and Li^+ is bound to the negatively charged phosphate. A red-shift of phosphate band is thus observed as S_0 increases. As clearly shown in Figure 1a (orange curve), the band is slightly red-shifted when $S_0 < 0.5$. Above 0.5, the shift greatly increases to 14 cm^{-1} and the gel is formed, indicating that a strong $\text{Li}^+-\text{PO}_4^-$ interaction is the key responsible for the gel formation. The band shift keeps increasing to 28 cm^{-1} with increasing S_0 prior to phase separation. Note that above the gel range ($S_0 = 1.0$), although the viscosity sharply decreases, the band does not shift back. In other words, although the long cylindrical micelles are transformed into short ones, Li^+ remains firmly bound to the phosphate.

For other gel-inducing salts, LiBr, LiI, and NaI, considerable red-shifts of the phosphate band with increasing S_0 can all be seen. The red-shifts of LiBr and LiI mixtures are over 40 cm^{-1} , greater than that of LiCl mixture. LiI can even cause a band shift $\sim 10\text{ cm}^{-1}$ at a small S_0 (Figure 1c). For the salts that slightly increase the viscosity, i.e., NaBr and KI, the bands of phosphate are found to slightly red-shift, too, over 5 cm^{-1} . For the salts that have no effect on the viscosity, i.e., NaCl, KCl, and KBr, the bands of the phosphate group are not changed either before phase separation at $S_0 = 0.5$. The shift of phosphate band perfectly matches with the change of viscosity, implying that the structural and rheological transition originate from the interactions between lecithin and alkali halides. By comparing the band shifts of phosphates caused by alkali bromides (Figures 1b, 1e, and 1h), the order $\text{Li}^+ > \text{Na}^+ > \text{K}^+$ for the binding strength of alkali cations with phosphate can be clearly distinguished. More importantly, by comparing sodium halide series (Figures 1d, 1e, and 1f), although it is the cation that binds the phosphate, the binding abilities of the cations are mediated by the paired anions, following the order $\text{I}^- > \text{Br}^- > \text{Cl}^-$.

3.3.2. Carbonyl Groups. In addition to phosphate groups, the absorption band of the carbonyl groups ($\text{C}=\text{O}$) on lecithin are also affected by the gel-inducing alkali halides. The $\text{C}=\text{O}$ stretching band of isolated lecithin molecules has been reported at 1744 cm^{-1} , which was measured in methanol.³¹ Figure 4b shows the $\text{C}=\text{O}$ bands of LiCl/lecithin mixture with varying S_0 . The $\text{C}=\text{O}$ band of pure lecithin in cyclohexane is found at 1740 cm^{-1} , lower than that of isolated lecithin. Pure lecithin in cyclohexane self-assembles into reverse micelles where lecithin molecules are organized in a closely packed manner, and the $\text{C}=\text{O}$ groups may form intermolecular dipole–dipole interactions. In other words, the 1740 cm^{-1} band observed in cyclohexane is the already red-shifted one from the lecithin molecules with dipole–dipole interactions.³¹ As S_0 is increased, the $\text{C}=\text{O}$ bands are further red-shifted though the shift is not as large as that of phosphate groups. We attribute the red-shift to a stronger dipole–dipole interaction caused by the binding of LiCl that holds lecithin molecules more tightly.²⁶

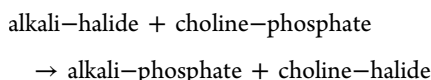
In Figure 1, the red curves show the changes of $\text{C}=\text{O}$ bands with S_0 for all the salts. Larger shifts can be found for the gel-inducing salts (LiCl, LiBr, LiI, and NaI), especially in the gel regions. As expected, NaBr and KI only give a very small shift with increasing S_0 while the effects of NaCl, KCl, and KBr are nearly undetectable. The dependence of $\text{C}=\text{O}$ band on the alkali halides is essentially the same as that of phosphate band but with a smaller shift. As will be elaborated in the Mechanism section, the tighter packing of lecithin molecules evidenced by the red-shift of $\text{C}=\text{O}$ bands is responsible for the structural transition of lecithin micelles. Furthermore, it is found that the shift of $\text{C}=\text{O}$ band shrinks above the gel region, especially for LiBr and LiI (Figures 1b and 1c), following the trend of viscosity. This suggests that the drop of viscosity is caused by a looser packing of lecithin molecules, though the cations are still firmly bound to phosphate.

3.3.3. Choline Groups. It has been reported that the absorption band of choline ($\text{CN}(\text{CH}_3)_3^+$) stretching depends weakly on solvents.⁴⁰ In Figure 4c, the choline group on pure lecithin in cyclohexane shows a band at 969 cm^{-1} . Interestingly, instead of the common red-shift, a blue-shift is found for the choline band when LiCl is incorporated, and the shift increases with S_0 . The opposite shift is attributed to a weaker association of Cl^- with the positively charged choline at the expense of the original stronger intra- and intermolecular choline–phosphate interaction. The shift of the choline band for all the salts as functions of S_0 is shown as the green curves in Figure 1. For the gel-inducing salts, the blue-shifts can be clearly seen and monotonically increase with S_0 , especially for LiBr and LiI. A small shift can also be detected for NaBr while no shift is found for the rest of the salts. The change of the choline band upon addition of alkali halides is mostly consistent with that of phosphate and $\text{C}=\text{O}$ bands discussed above.

By comparing all the data in Figure 1, the rheological property and the interaction between lecithin and alkali halides can be well correlated. Only the salts with strong ion–ion interaction with the headgroup of lecithin can greatly enhance the viscosity of the solutions and even induce the organogels, including LiCl, LiBr, LiI, and NaI. Although NaBr and KI show detectable interactions with lecithin from the FTIR measurements and the viscosities of the solutions are indeed increased, the interactions are not sufficiently strong to support the continuous growth of the lecithin micelles to form gels. For NaCl, KCl, and KBr, the interactions with lecithin are so weak that lecithin headgroup is unable to accommodate enough amounts of salts, and thus no effect is found prior to phase separation.

3.4. Mechanism. **3.4.1. Strength of Ion–Ion Interactions.** The S_0 for phase separation and the ability to induce gels reflect the strength of ion–ion interactions between alkali halides and lecithin. It is apparent that the valence is not the factor that matters. For the salts to take effect, the salts are required to dissociate into alkali cation and halide anion which then bind phosphate and choline, respectively. Therefore, the preference of the salts to dissociate or to remain in alkali–halide pair when mixed with lecithin is key to determine the effect of the salts. The dissociation of salts in water is common and is driven by the increase of entropy as well as the strong ion–water interactions. In our earlier study, residual water that is tightly bound to phosphate of lecithin had been determined by ^1H NMR at a molar ratio of water:lecithin = 0.9:1.²⁸ In the present organic systems with such a small quantity of water, the driving force for the dissociation of the salts must be different. The ion

exchange between alkali halides and lecithin phosphocholine headgroup can be regarded as the following reaction:



The occurrence of this reaction lies in the formation of energetically more stable alkali-phosphate and choline-halide pairs relative to the original state without dissociation, i.e., the alkali-halide and choline-phosphate pairs.

The strength of ion-ion interactions is dependent on the charge densities of the ions.²⁴ The ion pairs formed by cations and anions with higher charge densities is energetically favorable because the attraction force is stronger. Although all the ions are monovalent, their charge densities are different. Considering the electron affinity and the size of the ions, the charge density of the cations used in this study follows the order $\text{Li}^+ > \text{Na}^+ > \text{K}^+ > \text{CN}(\text{CH}_3)_3^+$ while that of the anions is in the order $\text{PO}_4^- > \text{Cl}^- > \text{Br}^- > \text{I}^-$.²⁵ The strength of Li^+ to bind PO_4^- is thus the highest, followed by Na^+ , K^+ and then $\text{CN}(\text{CH}_3)_3^+$, which is why the lithium salts are the most capable of inducing gels while the potassium salts are the least. This also explains the red-shifts of the phosphate band when the salts are bound to the headgroup as shown in Figure 1.

Another important question is why the types of halide anions affect the gel formation, especially for sodium salts, with the capability in the order $\text{I}^- > \text{Br}^- > \text{Cl}^-$. In the preceding FTIR section, the association of choline with halides instead of phosphate has been shown to be energetically unfavorable as evidenced by the blue-shift of the choline upon mixing with alkali halides (Figure 1). In other words, the ion exchange is not preferred for the halides and choline. Li^+ itself has a very strong interaction with PO_4^- so that the $\text{Li}^+-\text{PO}_4^-$ pair always forms regardless of the type of anion, similar to the effect of multivalent cations, such as Ca^{2+} and La^{3+} .²⁶ However, for the alkali cations that less strongly interact with PO_4^- , the effect of the halide anions becomes significant. Taking non-gel-inducing NaCl as an example, following the order of the charge density, $\text{Na}^+-\text{PO}_4^-$ interaction is stronger than Na^+-Cl^- . However, this energy favor is unable to compensate the energy disfavor when $\text{CN}(\text{CH}_3)_3^+-\text{PO}_4^-$ turns to be $\text{CN}(\text{CH}_3)_3^+-\text{Cl}^-$. Therefore, NaCl prefers not to dissociate to bind lecithin headgroups, especially at high S_0 where energy effect dominates. In the case of gel-inducing NaI, since the charge density of I^- is low, the $\text{Na}^+-\text{PO}_4^-$ pair is much more stable than the Na^+-I^- pair, which prevails the unfavorable $\text{CN}(\text{CH}_3)_3^+-\text{I}^-$ pair with respect to $\text{CN}(\text{CH}_3)_3^+-\text{PO}_4^-$. NaI thus tends to dissociate in lecithin headgroup and induce gels. The effect of Br^- is intermediate between Cl^- and I^- . For potassium salts, since K^+ has a weak interaction with phosphate, even I^- is unable to efficiently bring about the ion exchange. It is surprising that the ion interactions in the organic systems, such as the weak but favorable $\text{CN}(\text{CH}_3)_3^+-\text{I}^-$ binding,¹¹ are analogous to those in aqueous solutions where the interactions are strongly mediated by water, as described in the Introduction.^{1,11,17}

3.4.2. Structural Transition. The self-assembled structures of lecithin in cyclohexane depend on the molecular conformation that are affected by the interactions among lecithin, salts, and cyclohexane. The tails of lecithin tend to swell in cyclohexane, implying a larger tail area relative to headgroup area, and this leads to near-spherical reverse micelles based on the theory of critical packing parameter.⁴¹ The binding of salts to headgroups has two effects: first, as evidenced by C=O absorption bands,

the salts hold lecithin more tightly through the strong electrostatic interactions, and second, the interfacial tension between the hydrophilic cores and hydrophobic coronas increases because the salts and tail/cyclohexane are highly incompatible. The lecithin molecules, especially the tails, thus tend to straighten and densely pack to reduce the interfacial area between cores and coronas, in ways that transform spherical micelles into long cylindrical ones. The ionic binding of the salts to lecithin is expected to be stronger than hydrogen bonds such that the long cylindrical micelles are robust, analogous to rigid polymer chains with a long relaxation time. The solutions with networks formed by such cylindrical micelles thus behave like gels, different from conventional wormlike micellar solutions that are viscoelastic Maxwell fluids as the chains rapidly break and re-form through the exchange of amphiphiles between neighboring chains.⁴²

SANS modeling shows that not only the length but also the radius of the cylindrical micelles also slightly increases with increasing S_0 . This radial growth may result from the conformation change of both tails and headgroups on lecithin. As mentioned above, the binding salts force the tails to straighten and closely packed, which is the contribution of the tails to the increase of radius. In the reverse micelles of pure lecithin in low polar solvents, the positively charged choline group tend to fold back toward the negatively charged phosphate group to optimize the intra- and intermolecular interactions.⁴³ When the gel-inducing salts is incorporated in the headgroups, alkali cations replace choline to bind the phosphate group and the choline group no longer needs to fold back.⁴⁴ The headgroup thus adopts a more straightened conformation, making another contribution to the radius increase. The structural transition with increasing S_0 is depicted in Figure 5.

The reason why the viscosity drops above the gel region is not fully understood. The length of the cylindrical micelles should greatly reduce as S_0 exceeds a threshold ($S_0 \sim 1.0$), though such a length change is not seen from the SANS data at low concentration. If that is the case, the shortening of the micelles may be related to the conformation change of the headgroups. As discussed above, the binding of the salts straightens the choline in headgroups, which, in addition to the increase of radius, may decrease the effective cross-sectional area of phosphate and choline moieties. This molecular geometry change is favorable for forming curved structures like spherical micelles. Above the gel region, this effective area may be lowered to a critical level so that the long cylindrical micelles tend to break into short ones with more end-caps which are highly curved hemispheres and are thus thermodynamically more stable. The molecular packing in short cylindrical micelles, specifically the end-caps, is not as tight as that in long micelles, which can explain the recovery of the C=O band when S_0 exceeds the gel region, especially for LiBr and LiI as shown in Figures 1b and 1c.

4. CONCLUSIONS

This study has demonstrated that, in addition to the previously reported divalent and trivalent cations, monovalent alkali cations can alter the self-assembly of phospholipids like lecithin in low polar organic solvents. Divalent and trivalent cations interact strongly with phosphate of lecithin so that their effects are prominent regardless of the paired anions. However, for the alkali cations that weakly interact with lecithin, the paired anions play a decisive role. Strong effects are found in the case

of the alkali halides with cations of a higher charge density and with anions of a lower charge density, analogous to the ion–ion interactions found in aqueous systems. The salts with such a characteristic, including LiCl, LiBr, LiI, and NaI, strongly bind the headgroup of lecithin, change the molecular geometry, and then transform the original lecithin reverse spherical micelles to cylindrical micelles that are sufficiently long to form a quasi-permanent network, giving rise to the solidlike organogels. From this instance, we see that although water and low polar liquids are on opposite sides in terms of polarity, the effects of ions in these two systems are analogous, both following Hofmeister series. We would like to point out that there is only a thin line separates water and low polar liquids. The low polar solvents can provide a platform to study interactions occurring in biological systems where the measurements may be disturbed by the presence of water.

■ ASSOCIATED CONTENT

Supporting Information

The Supporting Information is available free of charge on the ACS Publications website at DOI: 10.1021/acs.langmuir.6b03449.

Figures S1–S14 (PDF)

■ AUTHOR INFORMATION

Corresponding Author

*E-mail: shtung@ntu.edu.tw (S.-H.T.).

Notes

The authors declare no competing financial interest.

■ ACKNOWLEDGMENTS

This work was financially supported by a joint grant from the Ministry of Science and Technology, Taiwan (MOST 103-2923-E-002-005-MY3) and the Russian Foundation for Basic Research (RFBR 14-03-92004-NNS_a). We acknowledge the support of the Australian Centre for Neutron Scattering, Australian Nuclear Science and Technology Organisation, in providing the neutron research facilities used in this work, and the support of NSRRC, Taiwan, for the travel expense of the neutron experiments (MOST 103-2739-M-213-001-MY3).

■ REFERENCES

- Berkowitz, M. L.; Vacha, R. Aqueous solutions at the interface with phospholipid bilayers. *Acc. Chem. Res.* **2012**, *45*, 74–82.
- Akutsu, H.; Seelig, J. Interaction of metal-ions with phosphatidylcholine bilayer-membranes. *Biochemistry* **1981**, *20*, 7366–7373.
- Altenbach, C.; Seelig, J. Ca²⁺ binding to phosphatidylcholine bilayers as studied by deuterium magnetic-resonance - Evidence for the formation of a Ca²⁺ complex with two phospholipid molecules. *Biochemistry* **1984**, *23*, 3913–3920.
- Marra, J.; Israelachvili, J. Direct measurements of forces between phosphatidylcholine and phosphatidylethanolamine bilayers in aqueous-electrolyte solutions. *Biochemistry* **1985**, *24*, 4608–4618.
- Huang, Y. X.; Tan, R. C.; Li, Y. L.; Yang, Y. Q.; Yu, L.; He, Q. C. Effect of salts on the formation of C₈-lecithin micelles in aqueous solution. *J. Colloid Interface Sci.* **2001**, *236*, 28–34.
- Bockmann, R. A.; Hac, A.; Heimburg, T.; Grubmuller, H. Effect of sodium chloride on a lipid bilayer. *Biophys. J.* **2003**, *85*, 1647–1655.
- Maity, P.; Saha, B.; Kumar, G. S.; Karmakar, S. Binding of monovalent alkali metal ions with negatively charged phospholipid membranes. *Biochim. Biophys. Acta, Biomembr.* **2016**, *1858*, 706–714.
- Bockmann, R. A.; Grubmuller, H. Multistep binding of divalent cations to phospholipid bilayers: A molecular dynamics study. *Angew. Chem., Int. Ed.* **2004**, *43*, 1021–1024.
- Cordomi, A.; Edholm, O.; Perez, J. J. Effect of ions on a dipalmitoyl phosphatidylcholine bilayer. A molecular dynamics simulation study. *J. Phys. Chem. B* **2008**, *112*, 1397–1408.
- Clarke, R. J.; Lupfert, C. Influence of anions and cations on the dipole potential of phosphatidylcholine vesicles: A basis for the Hofmeister effect. *Biophys. J.* **1999**, *76*, 2614–2624.
- Vacha, R.; Siu, S. W. I.; Petrov, M.; Bockmann, R. A.; Barucha-Kraszewska, J.; Jurkiewicz, P.; Hof, M.; Berkowitz, M. L.; Jungwirth, P. Effects of alkali cations and halide anions on the DOPC lipid membrane. *J. Phys. Chem. A* **2009**, *113*, 7235–7243.
- Pedersen, U. R.; Leidy, C.; Westh, P.; Peters, G. H. The effect of calcium on the properties of charged phospholipid bilayers. *Biochim. Biophys. Acta, Biomembr.* **2006**, *1758*, 573–582.
- Pabst, G.; Hodzic, A.; Strancar, J.; Danner, S.; Rappolt, M.; Laggner, P. Rigidification of neutral lipid bilayers in the presence of salts. *Biophys. J.* **2007**, *93*, 2688–2696.
- Edidin, M. Timeline - Lipids on the frontier: a century of cell-membrane bilayers. *Nat. Rev. Mol. Cell Biol.* **2003**, *4*, 414–418.
- Papahadjopoulos, D.; Nir, S.; Duzgunes, N. Molecular mechanisms of calcium-induced membrane-fusion. *J. Bioenerg. Biomembr.* **1990**, *22*, 157–179.
- Tillman, T. S.; Cascio, M. Effects of membrane lipids on ion channel structure and function. *Cell Biochem. Biophys.* **2003**, *38*, 161–190.
- Song, J.; Franck, J.; Pincus, P.; Kim, M. W.; Han, S. Specific ions modulate diffusion dynamics of hydration water on lipid membrane surfaces. *J. Am. Chem. Soc.* **2014**, *136*, 2642–2649.
- Kunz, W.; Henle, J.; Ninham, B. W. 'Zur Lehre von der Wirkung der Salze' (about the science of the effect of salts): Franz Hofmeister's historical papers. *Curr. Opin. Colloid Interface Sci.* **2004**, *9*, 19–37.
- Yang, Z. Hofmeister effects: an explanation for the impact of ionic liquids on biocatalysis. *J. Biotechnol.* **2009**, *144*, 12–22.
- Rydall, J. R.; Macdonald, P. M. Investigation of anion binding to neutral lipid-membranes using H-2 NMR. *Biochemistry* **1992**, *31*, 1092–1099.
- Garcia-Celma, J. J.; Hatahet, L.; Kunz, W.; Fendler, K. Specific anion and cation binding to lipid membranes investigated on a solid supported membrane. *Langmuir* **2007**, *23*, 10074–10080.
- Sachs, J. N.; Woolf, T. B. Understanding the Hofmeister effect in interactions between chaotropic anions and lipid bilayers: Molecular dynamics simulations. *J. Am. Chem. Soc.* **2003**, *125*, 8742–8743.
- Vacha, R.; Jurkiewicz, P.; Petrov, M.; Berkowitz, M. L.; Bockmann, R. A.; Barucha-Kraszewska, J.; Hof, M.; Jungwirth, P. Mechanism of interaction of monovalent ions with phosphatidylcholine lipid membranes. *J. Phys. Chem. B* **2010**, *114*, 9504–9509.
- Collins, K. D. Charge density-dependent strength of hydration and biological structure. *Biophys. J.* **1997**, *72*, 65–76.
- Collins, K. D. Ion hydration: Implications for cellular function, polyelectrolytes, and protein crystallization. *Biophys. Chem.* **2006**, *119*, 271–281.
- Lee, H. Y.; Diehn, K. K.; Ko, S. W.; Tung, S. H.; Raghavan, S. R. Can simple salts influence self-assembly in oil? Multivalent cations as efficient gelators of lecithin organosols. *Langmuir* **2010**, *26*, 13831–13838.
- Scartazzini, R.; Luisi, P. L. Organogels from lecithins. *J. Phys. Chem.* **1988**, *92*, 829–833.
- Tung, S. H.; Huang, Y. E.; Raghavan, S. R. A new reverse wormlike micellar system: Mixtures of bile salt and lecithin in organic liquids. *J. Am. Chem. Soc.* **2006**, *128*, 5751–5756.
- Hashizaki, K.; Chiba, T.; Taguchi, H.; Saito, Y. Highly viscoelastic reverse worm-like micelles formed in a lecithin/urea/oil system. *Colloid Polym. Sci.* **2009**, *287*, 927–932.
- Yang, G.; Zhao, J. X. From reverse worms to reverse vesicles formed by mixed zwitterionic and non-ionic surfactants in cyclohexane. *RSC Adv.* **2016**, *6*, 15694–15700.

- (31) Njauw, C. W.; Cheng, C. Y.; Ivanov, V. A.; Khokhlov, A. R.; Tung, S. H. Molecular interactions between lecithin and bile salts/acids in oils and their effects on reverse micellization. *Langmuir* **2013**, *29*, 3879–3888.
- (32) Zhang, J. Q.; Jin, J. Y.; Zou, L.; Tian, H. Reversible photo-controllable gels based on bithienylethene-doped lecithin micelles. *Chem. Commun.* **2013**, *49*, 9926–9928.
- (33) Sokolova, A.; Christoforidis, J.; Eltobaji, A.; Barnes, J.; Darmann, F.; Whitten, A. E.; de Campo, L. BILBY: Time-of-flight small angle scattering instrument. *Neutron News* **2016**, *27*, 9–13.
- (34) Kline, S. R. Reduction and analysis of SANS and USANS data using IGOR Pro. *J. Appl. Crystallogr.* **2006**, *39*, 895–900.
- (35) Pedersen, J. S. Analysis of small-angle scattering data from colloids and polymer solutions: modeling and least-squares fitting. *Adv. Colloid Interface Sci.* **1997**, *70*, 171–210.
- (36) Macosko, C. W. *Rheology: Principles, Measurements and Applications*; VCH Publishers: New York, 1994.
- (37) Raghavan, S. R.; Cipriano, B. H. Gel formation: Phase diagrams using tabletop rheology and calorimetry. In *Molecular Gels*; Weiss, R. G., Terech, P., Eds.; Springer: Dordrecht, 2005; pp 233–244.
- (38) Shervani, Z.; Jain, T. K.; Maitra, A. Nonconventional lecithin gels in hydrocarbon oils. *Colloid Polym. Sci.* **1991**, *269*, 720–726.
- (39) Shumilina, E. V.; Khromova, Y. L.; Shchipunov, Y. A. A study of the structure of lecithin organic gels by Fourier transform IR spectroscopy. *Russ. J. Phys. Chem.* **2000**, *74*, 1083–1092.
- (40) Zawisza, I.; Lachenwitzer, A.; Zamlynyy, V.; Horswell, S. L.; Goddard, J. D.; Lipkowski, J. Electrochemical and photon polarization modulation infrared reflection absorption spectroscopy study of the electric field driven transformations of a phospholipid bilayer supported at a gold electrode surface. *Biophys. J.* **2003**, *85*, 4055–4075.
- (41) Israelachvili, J. N. *Intermolecular and Surface Forces*, 3rd ed.; Academic Press: San Diego, 2011.
- (42) Cates, M. E. Reptation of living polymers - Dynamics of entangled polymers in the presence of reversible chain-scission reactions. *Macromolecules* **1987**, *20*, 2289–2296.
- (43) Hauser, H.; Pascher, I.; Pearson, R. H.; Sundell, S. Preferred conformation and molecular packing of phosphatidylethanolamine and phosphatidylcholine. *Biochim. Biophys. Acta, Rev. Biomembr.* **1981**, *650*, 21–51.
- (44) Brown, M. F.; Seelig, J. Ion-induced changes in head group conformation of lecithin bilayers. *Nature* **1977**, *269*, 721–723.